Munawwar Mohabuth, Andrei Kotousov, Ching-Tai Ng
Effect of uniaxial stress on the propagation of higher-order Lamb wave modes
International Journal of Non-Linear Mechanics, 2016; 86:104-111

Effect of Uniaxial Stress on the Propagation of Higher–Order Lamb Wave Modes

Munawwar Mohabuth[1*], Andrei Kotousov[1] and Ching-Tai Ng[2]

[1]School of Mechanical Engineering, The University of Adelaide, Adelaide, SA 5005, Australia.

[2]School of Civil, Environmental and Mining Engineering, The University of Adelaide, Adelaide, SA 5005, Australia.

*Corresponding author. Tel.: +61 8 8313 6385.

E-mail addresses: munawwar.mohabuth@adelaide.edu.au (M. Mohabuth), andrei.kotousov@adelaide.edu.au (A. Kotousov), alex.ng@adelaide.edu.au (C-T. Ng)

Abstract: On the basis of the non-linear theory of elasticity and the invariant based formulation developed by Ogden, we analyse the effect of homogeneous stress on the propagation of Lamb waves. Using the theory of incremental deformations superimposed on large deformations, we derive the equations governing the propagation of small amplitude waves in a pre-stressed plate. By enforcing traction-free boundary conditions at the surfaces of the plate, we further obtain the characteristic equations for symmetric and anti-symmetric Lamb wave modes and investigate the effect of stress on the phase velocity, i.e. the acoustoelastic effect. A comparison with experimental data exhibits a better correlation than previously published results. The outcomes of this study can be utilised in the development of new techniques for the measurement of applied stresses based on the acoustoelastic effect. In particular, a strong sensitivity of the phase velocity to the applied stress near the cut-off frequencies of higher-order Lamb wave modes is a very promising option, which seems to have been overlooked in previous studies.

Keywords: Acoustoelasticity, Lamb waves, Pre-stressed plates, Finite deformation, Dispersion.

1. Introduction

The study of wave propagation problems in pre-stressed media has been the subject of much research over the past century. However, early works in this area were restricted to linear elasticity and the effect of small deformations on the propagation of small amplitude waves; see, for example, the pioneering contribution by Biot (1940, 1965). It was not until the development of the finite deformation theory by Murnaghan (1937, 1951) that the non-linear effects of stresses were taken into account.

Two non-linear phenomena are associated with applied stresses: (1) a weak change of the local elastic behaviour of the material, and, (2) a weak non-linearity of the governing equations. As a result, the presence of initial stresses can have a substantial influence on the propagation of elastic waves in solids. In particular, these stresses affect the velocity, attenuation, dispersion and the non-linear aspects of the propagation of bulk waves. This interplay between the applied stress and the properties of the wave forms a conceptual foundation for the practical measurement of stresses in structural components.

The acoustoelastic effect is a non-linear phenomenon that describes the change in the speed of small amplitude waves in an elastic body due to the presence of a static pre-stress (Norris 2007). The theory of acoustoelasticity for bulk waves was initially developed by Hughes & Kelly (1953) who derived equations relating the wave velocity to the applied stress for isotropic materials subjected to uniaxial and hydrostatic loading. Their work was subsequently generalised by Toupin & Bernstein (1961) and Thurston & Brugger (1964) to materials of arbitrary crystal symmetry.

Acoustoelasticity is now a well-established procedure utilised in the non-destructive evaluation of applied and residual stresses. Its underlying principles have been comprehensively described in the reviews by Pao *et al.* (1983) and Guz & Makhort (2000). Ultrasonic bulk waves and the acoustoelastic effect have been used over the past sixty years in the measurement and control of residual stresses in welded structures and railroad rails, the tightening of bolts and the assessment of stress levels in bars as well as in multi-wire strands (Chaki & Bourse 2009).

Acoustoelastic procedures are largely based on the measurements of the time-of-flight of an ultrasonic pulse. However, the relative change in the phase velocity, which

is directly proportional to the applied stress, is small and therefore, measurements must be performed with very high accuracy. Nevertheless, the main obstacles in ultrasonic pulse techniques are the influences of the microstructure, composition gradients and plastic deformations on the phase velocity, which can all produce changes in the velocity comparable to those due to applied or residual stresses.

With the current ultrasonic testing procedures, it is virtually impossible to distinguish between applied and residual stresses as the length scales of the measurements are often comparable with the length scales of the residual stresses due to fabrication. The latter is normally related to the characteristic size of the cross-sectional area. The use of guided waves instead of bulk waves is promising because guided waves can propagate over distances much larger than the characteristic size of residual stresses. In particular, guided waves in plate-like structures, also known as Lamb waves, have been found to be sensitive to changes in structural properties, temperature and stress (Veidt & Ng 2011, Ng & Veidt 2012). Despite that, there has not been much research on the theory of acoustoelasticity in regards to Lamb waves.

The paper by Gandhi *et al.* (2012) provides a fairly comprehensive acoustoelastic formulation to analyse the effect of biaxial loading in initially isotropic plates. However, their work is restricted to small initial strains such that the elasticity tensor is obtained to the first order in the infinitesimal strain tensor. In the current work, we extend the framework developed by Ogden (1984) for incremental deformations superimposed on large deformations and utilise an invariant-based formulation of the strain-energy function. The wave propagation is considered as an infinitesimal deformation which is superimposed onto a finite static homogeneous deformation. The dispersion relations derived are similar to those obtained by Roxburgh & Ogden (1994) for a pre-stressed compressible elastic plate. However, the latter authors did not investigate the acoustoelastic effect but instead focused on vibration and stability phenomena.

In recent years, there have been several important contributions related to the derivation of dispersion relations for pre-stressed layers, albeit in a different context to acoustoelasticity. In particular, we mention the papers by Kaplunov *et al.* (2000, 2002a, 2002b) and Pichugin & Rogerson (2001, 2002) on the dynamic response of pre-stressed incompressible layers and the works of Nolde *et al.* (2004), Rogerson & Prikazchikova

(2009) and Kayestha *et al.* (2011) in the case of pre-stressed compressible layers. The main motivation behind these contributions was to derive asymptotic models to describe the wave motion in the long and short wave limits. The derivation of such models is highly desirable as they readily allow for the qualitative analysis of fundamental as well as higher-order wave modes. A detailed asymptotic analysis is beyond the scope of the current paper but the reader is pointed to the books by Berdichevsky (2009) and Kaplunov (1998) for a comprehensive discussion on the subject.

The aim of the current paper is to investigate the effect of pre-stress on the speed of propagation of Lamb waves. The work of Nolde *et al.* (2004) is the most relevant to the present study. The authors derive dispersion relations for wave propagation along a principal direction for a general strain energy function, expressed in terms of invariants of the left Cauchy-Green strain tensor. Motivated by the industrial application of rubber-like materials, numerical results are then presented for the neo-Hookean, Varga and Blatz-Ko strain energy functions. A similar approach is followed in the current paper but the strain energy function is expressed in terms of a different set of invariants. The paper is organised as follows. In Section 2, we review the equations governing incremental motions superimposed on a finite deformation and the constitutive equation for an isotropic hyperelastic pre-stressed solid. The characteristic equations for symmetric and anti-symmetric Lamb wave modes are then derived in Section 3 by considering the propagation of plane waves along the direction of the applied load and by enforcing traction-free boundary conditions at the surfaces of the plate. These equations are subsequently specialised in Section 4 to the case of weakly non-linear elasticity by considering the Murnaghan form of strain energy function, which is applicable to a large class of engineering materials. Finally, in Section 5, we solve these equations numerically and compare the dispersion results with previously published results and experimental data.

2. Governing Equations

The governing equations used in the theory of acoustoelasticity are briefly reviewed here based on the work of Destrade & Ogden (2012). First, we recall the equations for incremental motions and the constitutive equation for pre-stressed solid. Then, we consider an invariant based formulation of the strain energy function and provide an expression for the components of the elasticity tensor in terms of the

invariants. This general framework will be utilised to derive the dispersion relations for acoustoelastic Lamb wave propagation.

2.1 Incremental motions

Following the development by Ogden (2007), we consider an isotropic hyperelastic body of density ρ_r in some stress-free reference configuration, denoted by β_r. Suppose the body is subjected to a finite static pure homogeneous deformation, so that it occupies a new configuration, denoted by β_0, referred to as the deformed configuration. The corresponding deformation gradient relating β_r to β_0 is then given by $\mathbf{F} = \partial \boldsymbol{x}/\partial \boldsymbol{X}$, where $\boldsymbol{x}$ is the position vector in β_0 of a particle located at $\mathbf{X}$ in β_r. For a body without internal constraints, the nominal and Cauchy stress tensors are given by

$$\mathbf{S} = \frac{\partial W}{\partial \mathbf{F}}, \qquad \boldsymbol{\sigma} = J^{-1}\mathbf{F}\frac{\partial W}{\partial \mathbf{F}}, \tag{1}$$

respectively, where $\mathrm{W} = \mathrm{W}(\mathbf{F})$ is the strain energy function per unit reference volume and $J = \det \mathbf{F}$.

Next, we consider the superposition of a small-amplitude time-dependent motion upon the static finite deformation. It is then more convenient to use the deformed configuration β_0 as the reference configuration rather than the initial configuration β_r and for this purpose, we define $\boldsymbol{u}(\boldsymbol{x}, \mathrm{t})$ as the displacement vector relative to β_0. The corresponding incremental constitutive relation is given in component form by

$$\hat{\mathrm{S}}_{0_{pi}} = \mathcal{A}_{0_{piqj}}\, u_{j,q}\,, \tag{2}$$

where $\hat{\mathrm{S}}_{0_{pi}}$ are the components of the incremental nominal stress tensor, $\mathcal{A}_{0_{piqj}}$ are the components of the fourth-order elasticity tensor of instantaneous elastic moduli and a comma indicates partial differentiation with respect to the Eulerian coordinates.

The incremental governing equations of motion can be written in terms of the components of the elasticity tensor as

$$\mathcal{A}_{0piqj}\, u_{j,pq} = \rho \ddot{u}_i\,, \tag{3}$$

where $\rho = \rho_r J^{-1}$ is the density of the material in the deformed configuration β_0 and a superposed dot indicates partial differentiation with respect to time. The components of the elasticity tensor $\mathcal{A}_{0_{piqj}}$ can be expressed in terms of the strain energy function W as

$$\mathcal{A}_{0piqj} = J^{-1} F_{p\alpha} F_{q\beta} \frac{\partial^2 W}{\partial F_{i\alpha} \partial F_{j\beta}} \,, \tag{3}$$

and we note the major symmetry $\mathcal{A}_{0piqj} = \mathcal{A}_{0qjpi}$ (Destrade & Ogden 2012).

For a more comprehensive overview of the theory of incremental deformations superimposed on a finite deformation, we refer to Ogden (1984, 2007).

2.2 Invariant-based formulation

The strain-energy function W is required to be objective, which means that W depends on $\mathbf{F}$ only through the right Cauchy-Green deformation tensor, defined by $\mathbf{C} = \mathbf{F}^{\mathrm{T}}\mathbf{F}$. Since the material is also assumed to be isotropic relative to β_r, W can be expressed as a function of the principal invariants of $\mathbf{C}$, given by

$$I_1 = \mathrm{tr}\,\mathbf{C}, \qquad I_2 = \frac{1}{2}\left[(\mathrm{tr}\,\mathbf{C})^2 - \mathrm{tr}\left(\mathbf{C^2}\right)\right], \qquad I_3 = \det \mathbf{C}\,. \tag{5}$$

The nominal stress tensor and the elasticity tensor can be expanded out in terms of I_1, I_2 and I_3. These involve the computation of

$$\frac{\partial W}{\partial \mathbf{F}} = \sum_{i=1}^{3} W_i \frac{\partial I_i}{\partial \mathbf{F}}, \tag{6}$$

and

$$\frac{\partial^2 W}{\partial \mathbf{F}\,\partial \mathbf{F}} = \sum_{i=1}^{3} W_i \frac{\partial^2 I_i}{\partial \mathbf{F}\,\partial \mathbf{F}} + \sum_{i=1}^{3}\sum_{j=1}^{3} W_{ij} \frac{\partial I_i}{\partial \mathbf{F}} \otimes \frac{\partial I_j}{\partial \mathbf{F}} \,, \tag{7}$$

where $W_i = \partial W/\partial I_i$ and $W_{ij} = \partial^2 W/\partial I_i\,\partial I_j$. The expressions for the derivatives of the invariants, $\partial I_i/\partial \mathbf{F}$ and $\partial^2 I_i/\partial \mathbf{F}\partial \mathbf{F}$, were derived by Shams *et al.* (2011) and are not repeated here for brevity.

These expressions enable the nominal stress tensor, $\mathbf{S}$, to be written out as

$$\mathbf{S} = 2\,W_1\,\mathbf{F}^{\mathrm{T}} + 2\,W_2\,(I_1\mathbf{I} - \mathbf{C})\,\mathbf{F}^{\mathrm{T}} + 2\,I_3\,W_3\;\mathbf{F}^{-1}\,. \tag{8}$$

Similarly, the Cauchy stress tensor, $\boldsymbol{\sigma}$, is given by

$$J\,\boldsymbol{\sigma} = 2\,W_1\,\mathbf{B} + 2\,W_2\,(I_1\mathbf{B} - \mathbf{B}^2) + 2\,I_3\,W_3\,\mathbf{I}\ , \tag{9}$$

where $\mathbf{B} = \mathbf{F}\mathbf{F}^{\mathrm{T}}$ is the left Cauchy-Green deformation tensor. The elasticity tensor can also be expressed in terms of the derivatives of the invariants. In component form, it is given by

$$\begin{aligned} J\mathcal{A}_{0piqj} = \; & 2(W_1 + I_1W_2)\,B_{pq}\delta_{ij} \\ & + \; 2W_2\big[2B_{pi}B_{qj} - B_{iq}B_{jp} - B_{pr}B_{rq}\delta_{ij} - B_{pq}B_{ij}\big] \\ & + 2I_3W_3\big(2\delta_{ip}\delta_{jq} - \delta_{iq}\delta_{jp}\big) + 4W_{11}B_{ip}B_{jq} \\ & + \; 4W_{22}\big(I_1B_{ip} - B_{ir}B_{rp}\big)\big(I_1B_{jq} - B_{js}B_{sq}\big) \\ & + \; 4W_{12}\big(2I_1B_{ip}B_{jq} - B_{ip}B_{jr}B_{rq} - B_{jq}B_{ir}B_{rp}\big) \\ & + \; 4I_3W_{13}\big(B_{ip}\delta_{jq} + B_{jq}\delta_{ip}\big) \\ & + \; 4I_3W_{23}\big[I_1\big(B_{ip}\delta_{jq} + B_{jq}\delta_{ip}\big) - \delta_{ip}B_{jr}B_{rq} - \delta_{jq}B_{ir}B_{rp}\big] \\ & + \; 4I_3^2W_{33}\delta_{ip}\delta_{jq} \end{aligned} \tag{10}$$

where B_{ij} are the components of the left Cauchy-Green deformation tensor, $\mathbf{B}$. The above expression is the specialised form of the elasticity tensor for a pre-stressed isotropic elastic solid, given in Destrade & Ogden (2012). An equivalent expression can be found in Nolde *et al.* (2004) but we note that the latter authors have used a different set of invariants.

3. Acoustoelastic Lamb wave

The general framework described in Section 2 allows the acoustoelastic effect to be investigated by considering the propagation of plane waves in infinite media (Destrade & Ogden 2012). In this section, we shall extend this framework to study the propagation of Lamb waves in a pre-stressed plate, along the loading direction. The equations developed have the same canonical form as those derived by Nayfeh & Chimenti (1989) for Lamb waves propagating along the principal axes for materials of orthotropic or higher symmetry.

3.1 Uniform extension with lateral contraction

We consider an infinite isotropic plate of thickness D, with the reference Cartesian coordinate system $\mathbf{X} = (X_1, X_2, X_3)$ aligned as shown in Figure 1. The origin of the coordinate system lies at the mid-plane of the plate and the normal to the surface coincides with the X_2 axis of the coordinate system.

Suppose the plate is subjected to a pure homogeneous finite static deformation from the reference configuration. If the Lagrangian and Eulerian Cartesian basis vectors are chosen to coincide with the principal directions of the pre-strain, then the deformation can be expressed as

$$x_1 = \lambda_1 X_1, \qquad x_2 = \lambda_2 X_2, \qquad x_3 = \lambda_3 X_3 , \tag{11}$$

where $\lambda_1, \lambda_2, \lambda_3$ are the principal stretches. As a result, the deformation gradient tensor and the Cauchy-Green deformation tensors are given by $\mathbf{F} = \mathrm{diag}(\lambda_1, \lambda_2, \lambda_3)$ and $\mathbf{B} = \mathbf{C} = \mathrm{diag}\left(\lambda_1^{\,2}, \lambda_2^{\,2}, \lambda_3^{\,2}\right)$ respectively. The principal invariants of $\mathbf{C}$ thus reduce to

$$I_1 = \lambda_1^{\,2} + \lambda_2^{\,2} + \lambda_3^{\,2}, \qquad I_2 = \lambda_1^{\,2}\lambda_2^{\,2} + \lambda_2^{\,2}\lambda_3^{\,2} + \lambda_3^{\,2}\lambda_1^{\,2}, \qquad I_3 = \lambda_1^{\,2}\,\lambda_2^{\,2}\,\lambda_3^{\,2} . \tag{12}$$

We also note that, when referred to axes aligned with the principal axes of pre-strain, the only non-zero components of the elasticity tensor are given by $\mathcal{A}_{0iiii}, \mathcal{A}_{0iijj}, \mathcal{A}_{0ijij}$ and $\mathcal{A}_{0ijji}, i \neq j$ with $i, j \in \{1,2,3\}$ (Ogden 1984).

We now specialise the deformation to uniaxial tension and assume that the plate has been pre-stressed by the application of a Cauchy stress σ such that the plate is finitely deformed. Without loss of generality, we may take the uniaxial Cauchy stress σ to be along the x_1 axis, such that $\sigma_1 = \sigma$ and the corresponding principal stretch is λ_1. Since there is symmetry perpendicular to the x_1 axis, as the plate was considered to be isotropic in the absence of pre-stress, then λ_2 is equal to λ_3 (Ogden 1984).

For a given uniaxial stress field and strain energy function, the principal stretches can be determined by inverting the connection in equation (9) and using the expression in equation (12). The components of the elasticity tensor, $\mathcal{A}_{0piqj}$, can subsequently be determined using equation (10). In particular, we note that the uniaxial stress field leads to strain induced anisotropy, and as a result, the elastic response of the plate becomes transversely isotropic in nature (Destrade & Ogden 2012). However, the elasticity tensor does not possess the same symmetries as the elasticity tensor in the case of classical transversely isotropic linear elasticity.

3.2 Lamb Wave Dispersion Equation

The propagation of acoustoelastic Lamb waves for a homogeneous uniaxial stress field requires the equation governing incremental motions superimposed on a

finite deformation as given by equation (4) to be solved, in conjunction with stress-free boundary conditions at the surfaces of the plate.

In this paper, we restrict our attention to the plane strain incremental problem of wave propagation along the direction of the applied uniaxial stress only. The wave motion is modeled as

$$u_j = U_j e^{i\xi(x_1+\alpha x_2-ct)}\,, \qquad j = 1,2\,, \tag{13}$$

where u_j is the particle displacement, U_j is the amplitude of the displacement, ξ is the wavenumber along the x_1 direction, α is the ratio of the wavenumbers in the x_2 direction to that in the x_1 direction and c is the phase velocity in the x_1 direction. This general form represents plane waves, confined to the $x_1 - x_2$ plane, travelling with a velocity of c in the x_1 direction.

Substituting equation (13) into the equation of motion (4) yields an eigenvalue problem. Using tensor analysis, it is easy to see that $u_{j,pq}$ and $u_{i,tt}$ are given by

$$u_{j,pq} = (-\xi^2)(\beta_{pq})u_j\,, \tag{14}$$

and

$$u_{i,tt} = (-\xi^2)(c^2)\,u_j\delta_{ij} \tag{15}$$

respectively, where $\beta_{pq} = \begin{bmatrix} 1 & \alpha \\ \alpha & \alpha^2 \end{bmatrix}$ and δ_{ij} is the Kronecker delta function.

The eigenvalue problem can be expressed as

$$\left(\mathcal{A}_{0piqj}\beta_{pq} - \rho c^2\delta_{ij}\right)u_j = 0\,, \tag{16}$$

which is a form of the well-known Christoffel equation for anisotropic media (Rose 1999). Here, we define a modified form of the Christoffel acoustic tensor as

$$K_{ij} = \mathcal{A}_{0piqj}\beta_{pq} - \rho c^2\delta_{ij}. \tag{17}$$

Expanding the acoustic tensor, noting that i and j are free indices while p and q are summed over, yields

$$
\begin{aligned}
K_{11} &= \rho c^2 - \mathcal{A}_{01111} - \mathcal{A}_{02121}\alpha^2 \,, \\
K_{12} &= -\alpha(\mathcal{A}_{01122} + \mathcal{A}_{01221}) \,, \\
K_{21} &= -\alpha(\mathcal{A}_{01221} + \mathcal{A}_{01122}) \,, \\
K_{22} &= \rho c^2 - \mathcal{A}_{01212} - \mathcal{A}_{02222}\alpha^2 \,,
\end{aligned}
\tag{18}
$$

For non-trivial solutions to the eigenvalue problem, the determinant of the acoustic tensor must go to zero. This yields a fourth order equation in α which can be expressed as

$$
\mathrm{P}_4\,\alpha^4 + \mathrm{P}_2\,\alpha^2 + \mathrm{P}_0 \;= 0 \,, \tag{19}
$$

where the coefficients P_4 , P_2 and P_0 are given by

$$
\mathrm{P}_4 = \mathcal{A}_{02121}\mathcal{A}_{02222} \,,
$$

$$
\begin{aligned}
\mathrm{P}_2 = {} & -\rho c^2(\mathcal{A}_{02222} + \mathcal{A}_{02121}) + \mathcal{A}_{02222}\mathcal{A}_{01111} + \mathcal{A}_{02121}\mathcal{A}_{01212} \\
& - \mathcal{A}_{01122}\mathcal{A}_{01221} - \mathcal{A}_{01122}\mathcal{A}_{01122} - \mathcal{A}_{01221}\mathcal{A}_{01221} \\
& - \mathcal{A}_{01221}\mathcal{A}_{01122} \,,
\end{aligned}
\tag{20}
$$

$$
\mathrm{P}_0 = \rho^2 c^4 - \rho c^2(\mathcal{A}_{01212} + \mathcal{A}_{01111}) + \mathcal{A}_{01111}\mathcal{A}_{01212} \,,
$$

The lack of odd power coefficients in equation (19) means that the fourth order equation can be reduced to a quadratic equation in α^2. This simplification results in four solutions for α, which are denoted by α_q, $q \in \{1,2,3,4\}$, with the following properties

$$
\alpha_2 = -\alpha_1, \qquad \alpha_4 = -\alpha_3 \,. \tag{21}
$$

These solutions correspond to four partial waves in the $x_1 - x_2$ plane which superpose to form Lamb waves.

In order to satisfy the stress-free boundary conditions, we follow the approach in Nayfeh & Chimenti (1989) and define the displacement ratio of U_2 to U_1 for each of the four values of α. Using the relations in equation (21), the displacement ratio for each α_q can be expressed as a function of the wave velocity and the material properties as

$$
W_q = \frac{(\rho c^2 - \mathcal{A}_{01111} - \mathcal{A}_{02121}\alpha_q^2)}{\alpha_q(\mathcal{A}_{01122} + \mathcal{A}_{01221})}, \qquad q \in \{1,2,3,4\}. \tag{22}
$$

The displacement field of the Lamb waves can then be written in terms of the

displacement ratio (22) by using the principle of superposition

$$u_1 = \sum_{q=1}^{4} U_1(\alpha_q) e^{i\xi(x_1+\alpha_q x_2-ct)} \ ,$$
$$u_2 = \sum_{q=1}^{4} U_1(\alpha_q) W_q e^{i\xi(x_1+\alpha_q x_2-ct)} \ . \tag{23}$$

Similarly, the stress field can be found by substituting the above displacement field into the incremental stress-displacement relations (2). The stress components in the x_2 direction are of interest

$$\hat{\mathrm{S}}_{022} = \sum_{q=1}^{4} i\xi D_{1q} U_1(\alpha_q) e^{i\xi(x_1+\alpha_q x_2-ct)} \ ,$$
$$\hat{\mathrm{S}}_{021} = \sum_{q=1}^{4} i\xi D_{2q} U_1(\alpha_q) e^{i\xi(x_1+\alpha_q x_2-ct)} \ , \tag{24}$$

where

$$D_{1q} = \mathcal{A}_{01122} + \alpha_q \mathcal{A}_{02222} W_q \ ,$$
$$D_{2q} = \mathcal{A}_{02121} \alpha_q + \mathcal{A}_{01221} W_q \ . \tag{25}$$

Incorporating the relations in (21) in equations (22), (23), (24) and (25) results in the following restrictions

$$W_{j+1} = -W_j \ ,$$
$$D_{1j+1} = D_{1j} \ , \tag{26}$$
$$D_{2j+1} = -D_{2j}, \qquad j = 1,3 \ .$$

In order to satisfy the incremental traction-free boundary conditions at the upper and lower surfaces of the plate, the components of the incremental nominal stress must be set to zero

$$\hat{\mathrm{S}}_{022} = \hat{\mathrm{S}}_{021} = 0 \text{ at } x_2 = \frac{\pm\lambda_2 D}{2} = \frac{\pm d}{2} \ . \tag{27}$$

This leads to four equations which can be expressed as

$$i\xi \begin{pmatrix} D_{11}E_1 & D_{12}E_2 & D_{13}E_3 & D_{14}E_4 \\ D_{21}E_1 & D_{22}E_2 & D_{23}E_3 & D_{24}E_4 \\ D_{11}\overline{E_1} & D_{12}\overline{E_2} & D_{13}\overline{E_3} & D_{14}\overline{E_4} \\ D_{21}\overline{E_1} & D_{22}\overline{E_2} & D_{23}\overline{E_3} & D_{24}\overline{E_4} \end{pmatrix} \begin{pmatrix} U_{11} \\ U_{12} \\ U_{13} \\ U_{14} \end{pmatrix} e^{i\xi(x_1 - ct)} = \begin{Bmatrix} 0 \\ 0 \\ 0 \\ 0 \end{Bmatrix}, \tag{28}$$

where $U_{1q} = U_1(\alpha_q), E_q = e^{i\xi\alpha_q\frac{d}{2}}$ and $\overline{E_q} = e^{-i\xi\alpha_q\frac{d}{2}}$. For non-trivial solutions, the determinant of the coefficient matrix in (28) must go to zero. Finally, using row and column operations along with the symmetries in (26), the determinant can be reduced to two characteristic equations

$$\begin{aligned} D_{11}D_{23}\cot(\gamma\alpha_1) - D_{13}D_{21}\cot(\gamma\alpha_3) = 0\,, \\ D_{11}D_{23}\tan(\gamma\alpha_1) - D_{13}D_{21}\tan(\gamma\alpha_3) = 0\,, \end{aligned} \tag{29}$$

corresponding to the symmetric and anti-symmetric Lamb wave modes respectively, with $\gamma = \xi d/2 = \omega d/2c$, ω being the angular frequency of the wave.

4. Weakly non-linear elasticity

In the theory of incremental deformations superimposed on a finite deformation, the amplitude of the wave motion is assumed to be infinitesimal. However, no restriction is placed on the magnitude of the finite deformation, or on the choice of the strain energy function W. To allow for small but finite effects, the strain energy function is specialised to weakly non-linear elasticity (Landau & Lifshitz 1986), whereby W is expressed as a power series in terms of a particular form of the strain tensor.

In the linear theory of elasticity, the strain energy function is of second order in the strain. However, to study the non-linear behaviour of materials, the strain energy function needs to be expanded to a higher order in the strain. In this paper, the non-linear effect of interest is the acoustoelastic effect and we aim to determine the second order correction to the wave speed. Thus, the strain energy function is expanded to the third order in the strain tensor and it is typically the Green-Lagrange strain tensor, given by $\mathbf{E} = \frac{1}{2}(\mathbf{C} - \mathbf{I})$, which is employed.

A well-known form of the third-order expanded strain energy function is that due to Murnaghan (1937, 1951)

$$W = \frac{1}{2}(\lambda + 2\mu)i_1^2 - 2\mu i_2 + \frac{1}{3}(l + 2m)i_1^3 - 2m\, i_1 i_2 + n i_3, \tag{31}$$

where i_1, i_2, i_3 are the principal invariants of $\mathbf{E}$, given by $i_1 = \mathrm{tr}\mathbf{E}$, $i_2 = \frac{1}{2}[i_1^2 - \mathrm{tr}(\mathbf{E})^2]$ and $i_3 = \det \mathbf{E}$ respectively. The parameters λ and μ are the classical Lamé elastic constants and l, m, n are the Murnaghan or third-order elastic constants. The Murnaghan model has been widely utilised to describe the behaviour of a large class of engineering materials, particularly in studies of wave propagation (Rushchitsky 2014). This is because the model takes into account material non-linearity through the presence of the third-order terms. The latter allow various non-linear effects, including acoustoelasticity, to be readily investigated.

In the present work, we shall use a particular form of Murnaghan's expansion, expressed in terms of the principal invariants of $\mathbf{C}$ instead of the principal invariants of $\mathbf{E}$ (Shams *et al.* 2011)

$$\begin{aligned} W = {} & \frac{\lambda}{8}(I_1 - 3)^2 + \frac{\mu}{4}\left({I_1}^2 - 2I_1 - 2I_2 + 3\right) + \frac{l}{24}(I_1 - 3)^3 \\ & + \frac{m}{12}(I_1 - 3)\left({I_1}^2 - 3I_2\right) + \frac{n}{8}(I_1 - I_2 + I_3 - 1)\,, \end{aligned} \tag{32}$$

where $I_1,\ I_2,\ I_3$ are the invariants previously defined in equation (5). For this particular strain energy function, the derivatives W_{13}, W_{22}, W_{23} and W_{33} turn out to be zero and thus, the expression for the elasticity tensor in equation (10) reduces to

$$\begin{aligned} J\mathcal{A}_{0piqj} = {} & 2(W_1 + I_1 W_2)\, B_{pq}\delta_{ij} \\ & + 2W_2\left[2B_{pi}B_{qj} - B_{iq}B_{jp} - B_{pr}B_{rq}\delta_{ij} - B_{pq}B_{ij}\right] \\ & + 2I_3 W_3\left(2\delta_{ip}\delta_{jq} - \delta_{iq}\delta_{jp}\right) + 4W_{11}B_{ip}B_{jq} \\ & + 4W_{12}\left(2I_1 B_{ip}B_{jq} - B_{ip}B_{jr}B_{rq} - B_{jq}B_{ir}B_{rp}\right). \end{aligned} \tag{33}$$

For a given (Cauchy) uniaxial stress field, the principal stretches can be determined by solving equation (9) along with equations (12) and (32). The components of the elasticity tensor, $\mathcal{A}_{0piqj}$, used in the dispersion relations can then be obtained using equation (33).

5. Selected Results

In this section, we present selected numerical results obtained by solving the analytical equations (29) using the algorithm developed by Gandhi (2010). The adopted

approach was verified by comparing the numerical results with the asymptotic solutions by Nolde *et al*. (2004) for specific ranges of frequencies, namely low, high and near cut-off frequency ranges. The material considered in this study is 6061-T6 Aluminium, which was chosen in order to make contact with previously published analytical predictions and experimental data from Gandhi *et al*. (2012). The material properties of the 6061-T6 Aluminium were sourced from Asay & Guenther (1967) and are listed in Table 1.

Figure 2 shows the dispersion curves for an aluminium plate subjected to a uniaxial stress of 100 MPa in tension (continuous line) and in compression (dashed line). The direction of propagation of the waves was chosen to be parallel to the applied load, as it was shown to exhibit the highest sensitivivity of the phase velocity to the applied stress in the case of longitudinal waves (Egle & Bray 1976). The shear horizontal modes are not shown here as they decouple from the Lamb wave modes. At this scale, the change in the phase velocity is not immediately obvious. However, it can be seen that, in general, the phase velocity seems to be higher for the compressive load as compared to the tensile load. This finding is consistent with the results of bulk wave acoustoelasticity which predicts that compressive stresses cause an increase in the phase velocity while tensile stresses lead to a decerease in the phase velocity (Hughes & Kelly 1953).

The change in the phase velocity for different symmetric and anti-symmetric Lamb wave modes at varying magnitudes of tensile stress is compared in Figure 3. For reasons of clarity, the results for compressive stresses are not shown here as they only demonstrate an opposite trend to the results obtained for tensile stresses. Figure 3 (a) shows the change in the phase velocity, compared to the unstressed state, of the fundamental symmetric mode (S0) as a function of the magnitude of the applied tensile load. It can be seen that the change in the phase velocity is negative for all the values of applied stress considered, which means that tensile stresses cause a decrease in the phase velocity of the S0 mode. Higher magnitudes of the applied stress result in larger changes in the phase velocity, particularly in the low frequency-thickness region. However, at higher frequency-thickness values, the change in the phase velocity tends to a constant value. This is not surprising since the S0 mode converges to the Rayleigh wave velocity at higher frequencies (Rose 1999).

The results for the fundamental anti-symmetric mode (A0), shown in Figure 3(b), are very intriguing. At low frequency-thickness values (500–5000 Hz-m), the change in the phase velocity is negative. At higher frequency-thickness values (above 5000 Hz-m), the change in the phase velocity tends to a constant value as the A0 mode also converges to the Rayleigh wave velocity (Rose 1999). However, at very low frequency-thickness values, a different trend is observed; the change in the phase velocity is positive and seems to be inversely proportional to the applied load. The inset plot in Figure 3 (d) shows a particularly interesting behaviour at a frequency-thickness product of approximately 380 Hz-m; it predicts that the change in the phase velocity is zero and, more importantly, is independent of the magnitude of the applied stress. This behaviour seems to be analogous to the isotropic phase velocity observed by Gandhi *et al.* (2012) for the A0 mode at varying angles of propagation.

The change in the phase velocity for higher Lamb wave modes is shown in Figures 3(c) S1 mode, 3(d) A1 mode, 3(e) S2 mode and 3(f) A2 mode. At high frequency-thickness values, the higher order modes exhibit a similar behaviour to the fundamental modes as the change in the phase velocity tends to constant value. This is because the higher order modes converge to the transverse wave velocity at high frequencies (Rose 1999). However, when the excitation frequency is near the cut-off frequency of the higher order modes, the change in the phase velocity is much higher than for the S0 mode across all frequencies, including the low frequency range. Previous efforts on the utilisation of the acoustoelastic effect for stress monitoring have mainly focused on the fundamental symmetric (S0) mode as well as bulk waves. The findings here suggest that the use of higher order Lamb wave modes with an excitation frequency near the cut-off frequency appears to be more advantageous due to the much higher sensitivity of the phase velocity to the applied stress.

Next, we compare the change in the phase velocity with both the theoretical and experimental results presented by Gandhi *et al.* (2012). The latter utilised an aluminium plate of thickness 6.35 mm which was subjected to uniaxial loads in the range 0 to 57.5 MPa. The experiments were conducted at three specific values of frequency, corresponding to three different modes, namely the S0 mode at 250 kHz, the S1mode at 600 kHz and and the A1 mode at 400 kHz. Referring to Figure 4, the analytical results from the present study show that a better agreement with the experimental values as compared to the theoretical results predicted by Gandhi *et al.* (2012). For lower values

of the applied stress, the analytical results are in excellent agreement with the experimental results, particularly in the case of the symmetric modes shown in Figures 4 (a) and (b). For higher values of the applied stress, the difference in the values is larger but is still within reasonable agreement. Gandhi *et al.* (2012) attributed the differences between their theoretical results and the experimental data to the difficulties in evaluating the third order elastic constants accurately. The same argument is also applicable to explain the discrepancy between the present results and the experimental data. Furthermore, we note that the discrepancy is also due to the fact that the experimental phase velocity changes determined by Gandhi *et al.* (2012) were calculated in the undeformed coordinate system. However, the phase velocities in the stressed and unstressed configurations are, in general, different due to the stretching of the material when it is subjected to a an applied stress.

6. Concluding Remarks

We have considered the problem of Lamb wave propagation in an initially isotropic elastic plate subjected to a homogeneous uniaxial stress field. The derived governing equations of motion and dispersion equations are based on the non-linear theory of elasticity and utilises an invariant-based formulation of the strain-energy function. New results are presented for the Murnaghan form of the strain energy function, which is applicable to a large class of engineering materials. The results correlate better with the considered experimental data than previously published numerical results. The theoretical predictions show the same tendencies as the experimental data and demonstrate that the phase velocity decreases with an increase in the magnitude of tensile stress.

The acoustoelastic effect for aluminium plates subjected to a realistic level of applied stresses (below 100 MPa) is quite significant, specifically below approximately 3000 Hz-m for fundamental symmetric mode. It is, however, much stronger for higher order modes near the cut-off frequencies. Combining the high sensitivity of the phase velocity to applied stresses with the excellent ability of Lamb waves to propagate over large distances without decay, the obtained theoretical equations can form a foundation for practical techniques to measure stresses in plate-like structures. Similar analytical dispersion equations can also be obtained for other simple geometries such as circular rods. In this case, the wave modes are described by the Pochhammer-Chree

characteristic equations (Chaki & Bourse 2009). However, an analysis of the dispersion equations for more complicated waveguides such as rail-tracks will require the use of numerical tools, including Finite Element Analysis.

One of the promising aspects of the experimental techniques based on the theory of acoustoelasticity, specifically for guided wave propagation in slender structures, is a possibility to distinguish between the residual (built-in) stresses and the applied stresses. This is possible because the characteristic length of residual stresses, which is normally related to the characteristic size of the cross-sectional area, is much smaller than the propagation distances of guided waves. Therefore, the influence of residual stresses on wave propagation in slender structures, such as rail-tracks, is likely to decay with distance due to their self-equilibrating nature (no bulk stress).

Acknowledgement

The work was supported by the Australian Research Council through Discovery Project DP160102233 and by the Department of Further Education, Employment, Science & Technology, Government of South Australia, under Catalyst Research Grant Program. Their support is greatly appreciated.

References

Asay, JR & Guenther, AH 1967, 'Ultrasonic studies of 1060 and 6061-T6 aluminum', *Journal of Applied Physics*, vol. 38, pp. 4086–4088.

Berdichevsky, VL 2009, *Variational Principles of Continuum Mechanics*, Interaction of Mechanics and Mathematics, Springer-Verlag Berlin Heidelberg.

Biot, MA 1940, 'The influence of initial stress on elastic waves', *Journal of Applied Physics*, vol. 11, pp. 522-530.

Biot, MA 1965, *Mechanics of Incremental Deformations*, John Wiley, New York.

Chaki, S & Bourse, G 2009, 'Guided ultrasonic waves for non-destructive monitoring of the stress levels in prestressed steel strands', *Ultrasonics*, vol. 49, pp. 162-171.

Destrade, M & Ogden, RW 2012, 'On stress-dependent elastic moduli and wave speeds', *IMA Journal of Applied Mathematics*, vol. 78, pp. 965-997.

Egle, DM & Bray, DE 1976, 'Measurement of acoustoelastic and third-order elastic constants for rail steel', *Journal of the Acoustial Society of America*, vol. 60, pp. 741–744.

Gandhi, N 2010, 'Determination of dispersion curves for acoustoelastic lamb wave propagation', MS Thesis, Georgia Institute of Technology, Atlanta.

Gandhi, N, Michaels, JE & Lee, SJ 2012, 'Acoustoelastic Lamb wave propagation in biaxially stressed plates', *Journal of the Acoustical Society of America*, vol. 132, pp. 1284-1293.

Guz, AN & Makhort, FG 2000, 'The physical fundamentals of the ultrasonic nondestructive stress analysis of solids', *International Applied Mechanics*, vol. 36, no. 9, pp. 1119-1149.

Hughes, D & Kelly, J 1953, 'Second-Order Elastic Deformation of Solids', *Physical Review*, vol. 92, pp. 1145-1149.

Kaplunov, JD, Kossovich, LY & Nolde, EV 1998, *Dynamics of Thin Walled Elastic Bodies*, Academic Press, San Diego.

Kaplunov, JD, Nolde, EV & Rogerson, GA 2000, 'A low-frequency model for dynamic motion in pre-stressed incompressible elastic structures', *Proceedings of the Royal Society of London A: Mathematical, Physical and Engineering Sciences*, vol. 456, pp. 2589–2610.

Kaplunov, JD, Nolde, EV & Rogerson, GA 2002a, 'An asymptotically consistent model for long-wave high-frequency motion in a pre-stressed elastic plate', *Mathematics and Mechanics of Solids*, vol. 7, pp. 581–606.

Kaplunov, JD, Nolde, EV & Rogerson, GA 2002b, 'Short wave motion in a pre-stressed incompressible elastic plate', *IMA Journal of Applied Mathematics*, vol. 67, pp. 383–399.

Kayestha, P, Wijeyewickrema, A & Kishimoto, K 2011, 'Wave propagation along a non-principal direction in a compressible pre-stressed elastic layer', *International Journal of Solids and Structures*, vol. 48, pp. 2141-2153.

Landau, LD & Lifshitz, EM 1986, *Theory of Elasticity*, Butterworth-Heinemann, Oxford.

Murnaghan, FD 1937, 'Finite Deformations of an Elastic Solid', *American Journal of Mathematics*, vol. 59, pp. 235-260.

Murnaghan, FD 1951, 'Finite deformation of an elastic solid', John Wiley & Sons, New York.

Nayfeh, AH & Chimenti, DE 1989, 'Free Wave Propagation in Plates of General Anisotropic Media', *Journal of Applied Mechanics*, vol. 56, pp. 881-886.

Ng, CT & Veidt, M 2012, 'Scattering characteristics of Lamb waves from debondings at structural features in composite laminates', *Journal of the Acoustical Society of America*, vol. 132, pp. 115-123.

Nolde, EV, Prikazchikova, LA & Rogerson, GA 2004, 'Dispersion of small amplitude waves in a pre-stressed, compressible elastic plate', *Journal of Elasticity*, vol. 75, pp. 1–29.

Norris, AN 2007, ‘Small-on-Large theory with applications to granular materials and fluid/solid systems’, in M. Destrade, G. Saccomandi (eds), *Waves in Nonlinear Pre-Stressed Materials*, Springer, Wien, pp. 27–62.

Ogden, RW 1984, *Non-Linear Elastic Deformations*, Ellis Horwood, Chichester.

Ogden, RW 2007, ‘Incremental statics and dynamics of pre-stressed elastic materials’, in M Destrade, G Saccomandi (eds), *Waves in Nonlinear Pre-Stressed Materials*, Springer, Wien, pp. 1–26.

Pao, YH, Sachse, W & Fukuoka, H 1983, ‘Acoustoelasticity and ultrasonic measurements of residual stresses’, *Physical Acoustics*, vol. 17, pp. 61-143.

Pichugin, AV & Rogerson, GA 2001, ‘A two-dimensional model for extensional motion of a pre-stressed incompressible elastic layer near cut-off frequencies’, *IMA Journal of Applied Mathematics*, vol. 66, pp. 357–385.

Pichugin, AV & Rogerson, GA 2002, ‘An asymptotic membrane-like theory for long wave motion in a pre-stressed elastic plate’, *Proceedings of the Royal Society of London A: Mathematical, Physical and Engineering Sciences*, vol. 458, pp. 1447–1468.

Rogerson, GA & Prikazchikova, LA 2009, ‘Generalisations of long wave theories for pre-stressed compressible elastic plates’, *International Journal of Non-Linear Mechanics*, vol. 44, pp. 520–529.

Roxburgh, DG & Ogden, RW 1994, ‘Stability and vibration of pre-stressed compressible elastic plates’, *International Journal of Engineering Science*, vol. 32, pp. 427–454.

Rose, JL 1999, *Ultrasonic Waves in Solid Media*, Cambridge University Press, Cambridge, United Kingdom.

Rushchitsky, JJ 2014, *Nonlinear Elastic Waves in Materials*, Foundations of Engineering Mechanics, Springer International Publishing.

Shams, M, Destrade, M & Ogden, RW 2011, ‘Initial stresses in elastic solids: Constitutive laws and acoustoelasticity’, *Wave Motion*, vol. 48, no. 7, pp. 552-567.

Thurston, RN & Brugger, K 1964, 'Third-order elastic constants and the velocity of small amplitude elastic waves in homogeneously stressed media', *Physical Review*, vol. 133, pp. A1604–A1610.

Toupin, RA & Bernstein, B 1961, 'Sound waves in deformed perfectly elastic materials. Acoustoelastic effect', *Journal of the Acoustical Society of America*, vol. 33, pp. 216–225.

Veidt, M & Ng, CT 2011, 'Influence of stacking sequence on scattering characteristics of the fundamental anti-symmetric Lamb wave at through holes in composite laminates', *Journal of the Acoustical Society of America*, vol. 129, pp. 1280-1287.

Figure

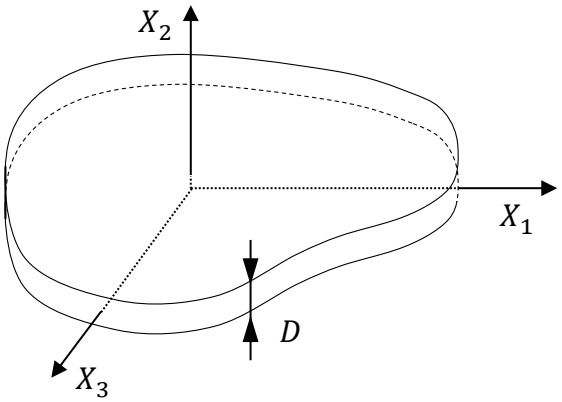

Figure 1: Alignment of the reference Cartesian coordinate system, with its origin lying at the mid-plane of the plate.

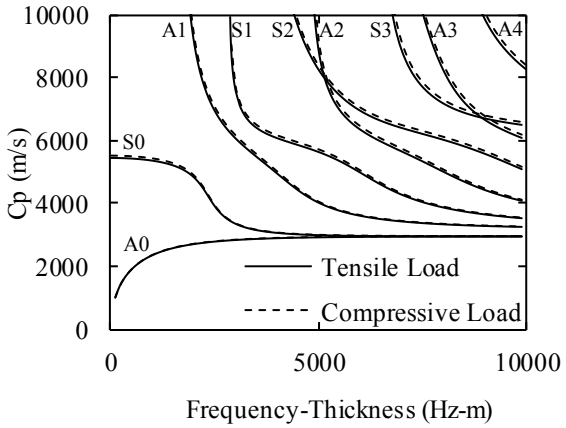

Figure 2: Dispersion curves for waves propagating in an Aluminium plate along the direction of a uniaxial applied stress of 100 MPa

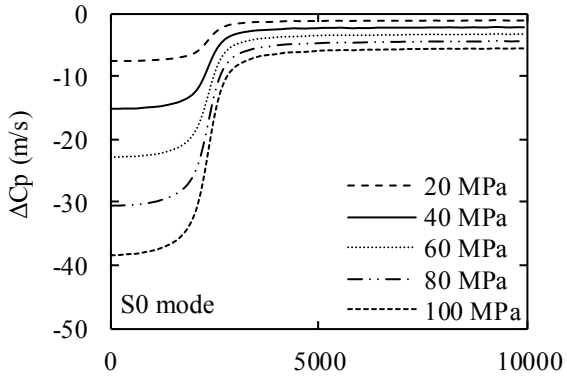
0
-10
-20
-30
-40
-50
ΔCp (m/s)
S0 mode
20 MPa
40 MPa
60 MPa
80 MPa
100 MPa
0
5000
10000
Frequency-Thickness (Hz-m)

(a)

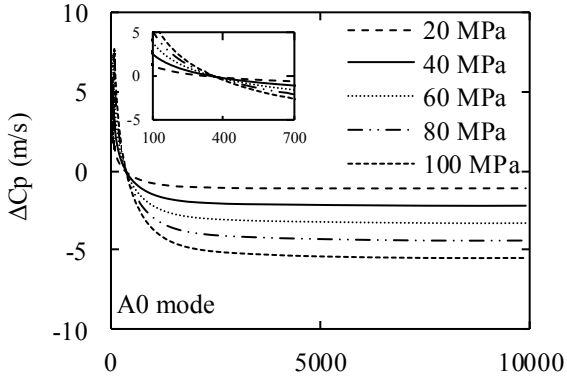
10
5
0
-5
-10
ΔCp (m/s)
A0 mode
20 MPa
40 MPa
60 MPa
80 MPa
100 MPa
5
0
-5
100
400
700
0
5000
10000
Frequency-Thickness (Hz-m)

(b)

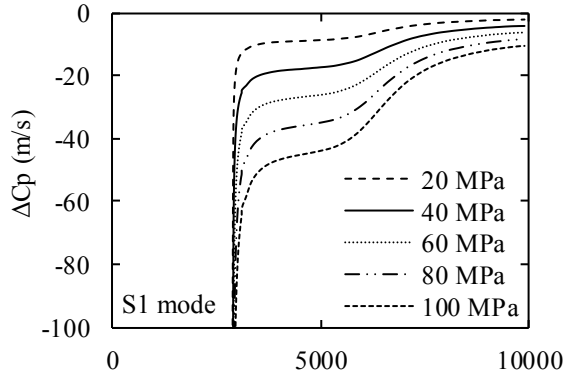
0
-20
-40
-60
-80
-100
ΔCp (m/s)
S1 mode
20 MPa
40 MPa
60 MPa
80 MPa
100 MPa
0
5000
10000
Frequency-Thickness (Hz-m)

(c)

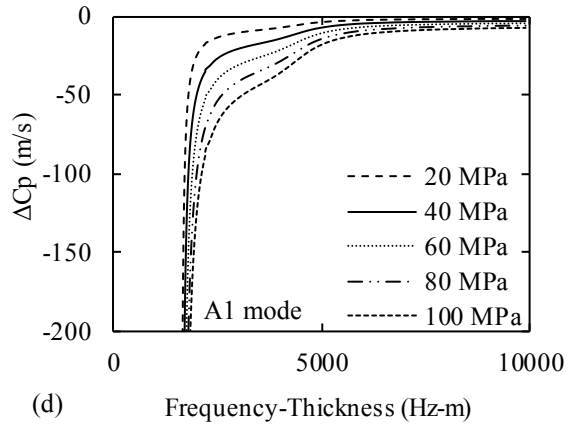

(d)

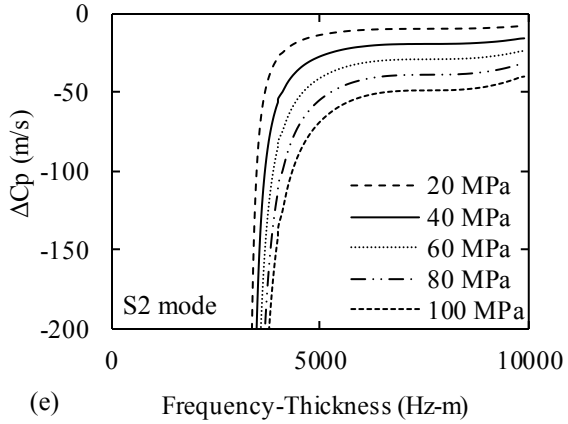

(e)

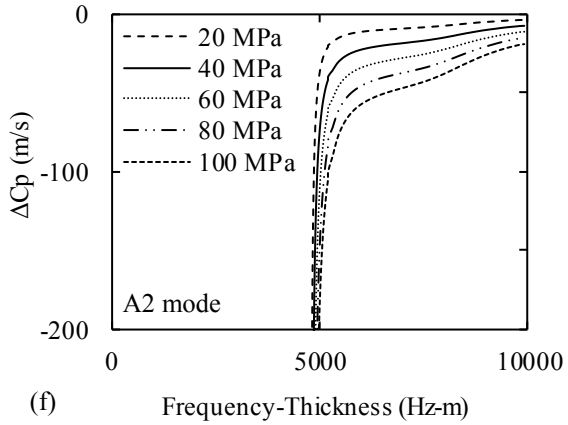

(f)

Figure 3: Change in phase velocity with Frequency-Thickness for modes propagating along the direction of uniaxial applied stress: (a) S0 mode, (b) A0 mode, (c) S1 mode, (d) A1 mode, (e) S2 mode and, (f) A2 mode.

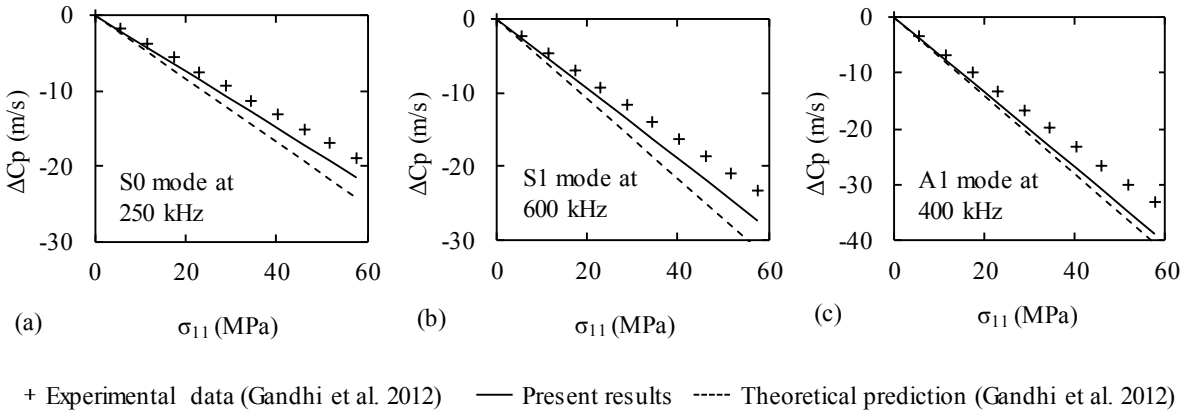

Figure 4: Comparison of the modelling outcomes of the present work with experimental results and theoretical predictions of a previous study. The results are presented for Lamb wave propagation in an Aluminium plate of thickness 6.35 mm along the direction of the uniaxial applied stress.

Table(s)

Table 1: Material Properties for 6061-T6 Aluminium

Elastic properties	Value
λ	54.308 GPa
μ	27.174 GPa
l	-281.5 GPa
m	-339.0 GPa
n	-416.0 GPa
ρ	2704 $\mathrm{kg/m^3}$